

Neural crest and Schwann cell progenitor-derived melanocytes are two spatially segregated populations similarly regulated by Foxd3

Erez Nitzan^a, Elise R. Pfaltzgraff^b, Patricia A. Labosky^{b,1}, and Chaya Kalcheim^{a,2}

^aDepartment of Medical Neurobiology, IMRIC and ELSC, Hebrew University-Hadassah Medical School, Jerusalem 91120, Israel; and ^bDepartment of Cell and Developmental Biology, Vanderbilt University Medical Center, Nashville, TN 37232-0494

Edited by Nicole M. Le Douarin, Centre National de La Recherche Scientifique, Gif-sur-Yvette, France, and approved June 28, 2013 (received for review April 4, 2013)

Skin melanocytes arise from two sources: either directly from neural crest progenitors or indirectly from neural crest-derived Schwann cell precursors after colonization of peripheral nerves. The relationship between these two melanocyte populations and the factors controlling their specification remains poorly understood. Direct lineage tracing reveals that neural crest and Schwann cell progenitor-derived melanocytes are differentially restricted to the epaxial and hypaxial body domains, respectively. Furthermore, although both populations are initially part of the Foxd3 lineage, hypaxial melanocytes lose Foxd3 at late stages upon separation from the nerve, whereas we recently found that epaxial melanocytes segregate earlier from Foxd3-positive neural progenitors while still residing in the dorsal neural tube. Gain- and loss-of-function experiments in avians and mice, respectively, reveal that Foxd3 is both sufficient and necessary for regulating the balance between melanocyte and Schwann cell development. In addition, Foxd3 is also sufficient to regulate the switch between neuronal and glial fates in sensory ganglia. Together, we propose that differential fate acquisition of neural crest-derived cells depends on their progressive segregation from the Foxd3-positive lineage.

DRG | Ednrb2 | MITF | pigment

All body melanocytes except the retinal pigment derive from the embryonic neural crest (NC), which in addition generates components of the peripheral nervous system, including sensory and autonomic neurons, satellite glia and Schwann cells (SCs), endocrine cells, and cranial mesectoderm (1, 2). The origins of pigment cells, their ancestral relationship to additional NC derivatives, and the mechanisms by which they segregate from each other remain poorly understood. Research in these areas is of fundamental importance for understanding aspects of pigment cell development as well as of adult physiology and pathology (3).

In the trunk of avian embryos, neural and melanocyte derivatives are sequentially produced after NC emigration from the dorsal neural tube (NT). The early migrating cells migrate in a dorsoventral direction to generate first the sympatho-adrenal primordium, then SC of the peripheral nerves; this is closely followed by cells that generate the dorsal root ganglia (DRG) (4–6). A day later, the last delaminating cells switch their pathway to migrate dorsolaterally through the nascent dermis. These cells give rise to melanocytes (4, 5, 7). In the NT, this continuous cell delamination is compensated for by a corresponding relocation of progenitors toward the dorsal area that constitutes a transition zone for the progressive influx and departure of cells. This dynamic behavior of dorsal NT progenitors is also reflected by the differential expression of at least three transcription factors, *Snail2*, *Sox9*, and *Foxd3*, in early neural progenitors and their down-regulation in the late subset of prospective melanoblasts, hence suggesting an early segregation between the precedent lineages (4, 5). Along this line, gain of Foxd3 activity in vivo induced the development of glial cells while inhibiting melanocytes, and conversely, genetic ablation of Foxd3 function

enhanced ectopic melanogenesis in the NT and later in DRG at the expense of both neurons and glia (8).

Adameyko et al. (9) found that SC progenitors (SCPs) lining elongating spinal nerves also constitute a source of pigment cells. These melanocytes differentiate at late stages relative to pigment cells directly generated from the NC. Thus, in addition to late emigrating/early differentiating NC-derived melanocytes, a subset of early delaminating NC cells that migrate dorsoventrally and later become SCs in association with the growing nerves can develop either into mature SCs if they remain in contact with nerve fibers or generate melanocytes if they detach from the nerve environment (3, 9, 10). Except for their common origin from the NC, the relationship between these two melanocyte subsets, at both cellular and molecular levels, remains to be elucidated. Not less intriguing is uncovering the downstream factors responsible for the switch between glial and melanocyte lineages. In vitro clonal analysis revealed the existence of single NC cells with melanocyte–glial potential (11), and further in vitro manipulations showed the plasticity of the differentiated melanocyte state (12). The mechanisms underlying this phenotypic conversion in the developing embryo are still obscure.

To begin investigating these questions, we asked whether the embryonic territories colonized by each melanocyte population are distinct or overlapping. Next we examined whether the nerve-derived SCP–melanocyte switch is regulated by Foxd3 as previously observed for melanocytes directly issued from the NC (8, 13, 14). Separate lineage tracing of each population revealed that NC and SCP-derived melanocytes are differentially restricted to the epaxial and hypaxial body domains, respectively, respecting the boundaries of the somite vs. lateral plate mesoderm-derived dermis through which they migrate. Furthermore, although both populations are initially part of the Foxd3 lineage, epaxial melanocytes segregate from Foxd3-positive neural progenitors already in the dorsal NT, whereas hypaxial melanocytes lose Foxd3 at late stages upon separation from the nerve. Gain- and loss-of-function experiments in avians and mice, respectively, reveal that Foxd3 is both sufficient and necessary for regulating the balance between melanocyte and SC development, similar to its role in epaxial melanocytes (8). Foxd3 is thus a negative regulator of both melanocyte populations. Because Foxd3 is also down-regulated in differentiating sensory neurons (15), we asked whether it plays a similar role during DRG development. When

Author contributions: E.N. and C.K. designed research; E.N. performed research; E.R.P. and P.A.L. contributed new reagents/analytic tools; E.N. and C.K. analyzed data; and E.N. and C.K. wrote the paper.

The authors declare no conflict of interest.

This article is a PNAS Direct Submission.

¹Present address: Office of Strategic Coordination, Division of Program Coordination, Planning, and Strategic Initiatives, Office of the Director, National Institutes of Health, Bethesda, MD 20892.

²To whom correspondence should be addressed. E-mail: kalcheim@cc.huji.ac.il.

This article contains supporting information online at www.pnas.org/lookup/suppl/doi:10.1073/pnas.1306287110/-DCSupplemental.

this normal down-regulation is prevented by conditional *Foxd3* overexpression in nascent DRG, neurogenesis is inhibited. Hence, a timely down-regulation of *Foxd3* is required for proper differentiation of both populations of NC-derived melanocytes as well as of NC-derived sensory neurons.

Results and Discussion

Dorsal Melanocytes Are Restricted to the Epaxial Domain of the Embryo, Whereas Ventral Melanocytes Primarily Colonize the Hypaxial Territory.

We characterized the relative domains colonized by “late emigrating, early differentiating” melanocytes directly issued from the NC and “early emigrating, late differentiating” melanocytes issued from NC-derived SCPs. To this end, a GFP-encoding DNA was electroporated into hemitubes of 35 somite stage (ss) embryos, a time when in the trunk, all ventrally migrating SCPs have already delaminated and only late-emigrating melanocytes are yet to leave the NT (5). Twenty-four hours later, at the limb level, labeled cells were present along the dorsolateral pathway, with the farthest cells reaching less than half-way between the dorsal midline and the ectodermal notch, an ectodermal/dermal indentation that subdivides epaxial from hypaxial domains of the embryonic body and serves as the limit between the somite and lateral plate-derived dermis, respectively (16–18) ($n = 9$; Fig. 1*A*, arrowhead). By 48 h, dorsal melanocytes reached the level of the ectodermal notch (Fig. 1*B*), which remained their ventral limit of migration even at 72 h, both at limb and flank levels of the axis ($n = 7$; Fig. 1*C* and *D*). To further examine whether the ectodermal notch is the ventral-most limit attained by NC-derived melanocytes in the flank, where this structure is less conspicuous, sections were examined for expression of *Sim-1*, a marker of somite-derived dermis, whose ventral limit of expression reaches the notch (17, 18). Indeed, GFP-labeled dorsal melanocytes, whether localized in dermis or ectoderm, did not migrate beyond the lateral-most *Sim1*-positive, epaxial domain of the body ($n = 4$; Fig. 1*D–D''*). Consistent with the precedent results, the majority of *Ednrb2* and *MC1*⁺ cells (5, 8) were apparent in the epaxial domain of the body at flank regions of embryonic day (E)5 embryos with very few pigment cells in the abdominal area at this stage (Fig. 1*E*, *G*, and *I*). In contrast to flank, at wing and hindlimb levels, total *Ednrb2* and *MC1*⁺ melanocytes were similarly distributed in both epaxial and hypaxial domains comprising the ectoderm and dermis of wings and limbs ($n = 5$ for each axial level; Fig. 1*F*, *H*, and *I*, $P < .05$ for hypaxial melanocytes in flank compared with limbs). To compensate for differences in surface area, we also determined the density of melanocytes in each domain; this measurement similarly showed that hypaxial melanocyte density is higher at limb compared with flank levels (Fig. 1*J*, $P < .05$). Together, this raised the questions of the origin of the hypaxial melanocytes and the precise embryonic territories they colonize.

Previously, SCP-derived melanocytes were reported to populate the limbs (3). Because our results show that NC-derived melanocytes are restricted to the epaxial body domain, we asked whether SCP-derived pigment is limited to the hypaxial domain or alternatively distributes throughout the dorsoventral body wall. To examine this issue, the dorsal NT was removed by cauterization at 35 ss at the hindlimb level after emigration of SCP but before delamination of NC-derived melanocytes (5), thus selectively eliminating the latter population. A day later, no dorsolaterally migrating melanocytes were apparent in the cauterized embryos compared with intact controls, and only few pigment cells were present close to the nerves in both intact and cauterized cases ($n = 6$ and 6; Fig. 2*A* and *B*). At E5.5, *Ednrb2*⁺ SCP-derived pigment cells populated the hindlimb region but were virtually absent from the epaxial domain located dorsal to the ectodermal notch ($n = 5$ and 11 for controls vs. cauterized; Fig. 2*C–E*, $*P < .05$). This suggests that at least until E5.5, NC and SCP-derived melanocytes are topographically segregated to epaxial and hypaxial body domains, respectively.

To further challenge this conclusion, we selectively and stably labeled the early ventrally migrating NC cells (i.e., prospective

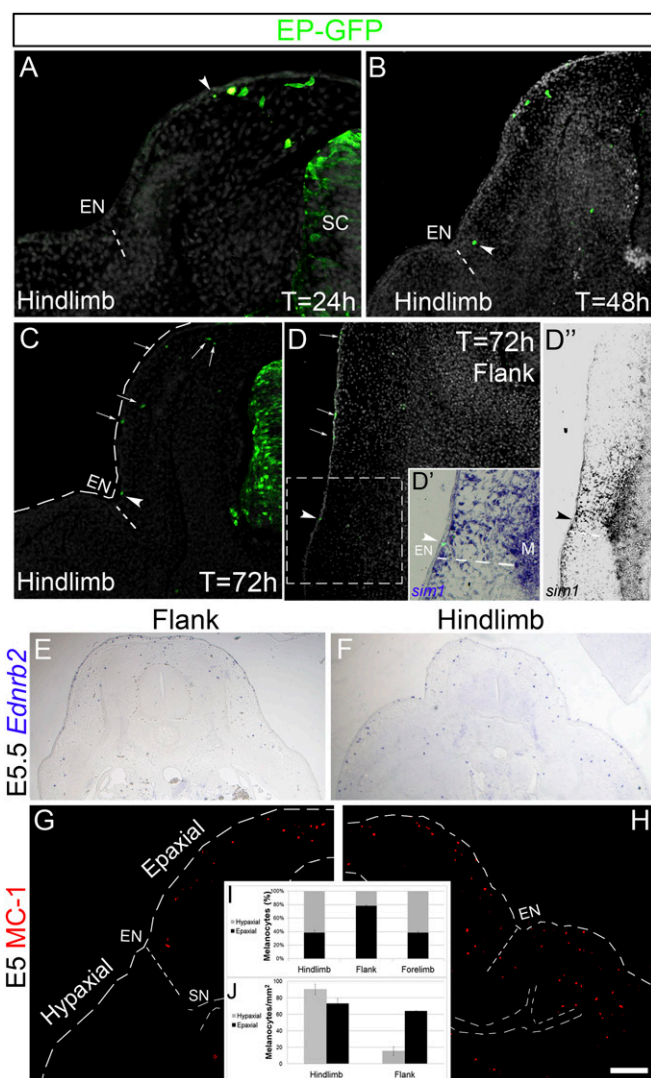
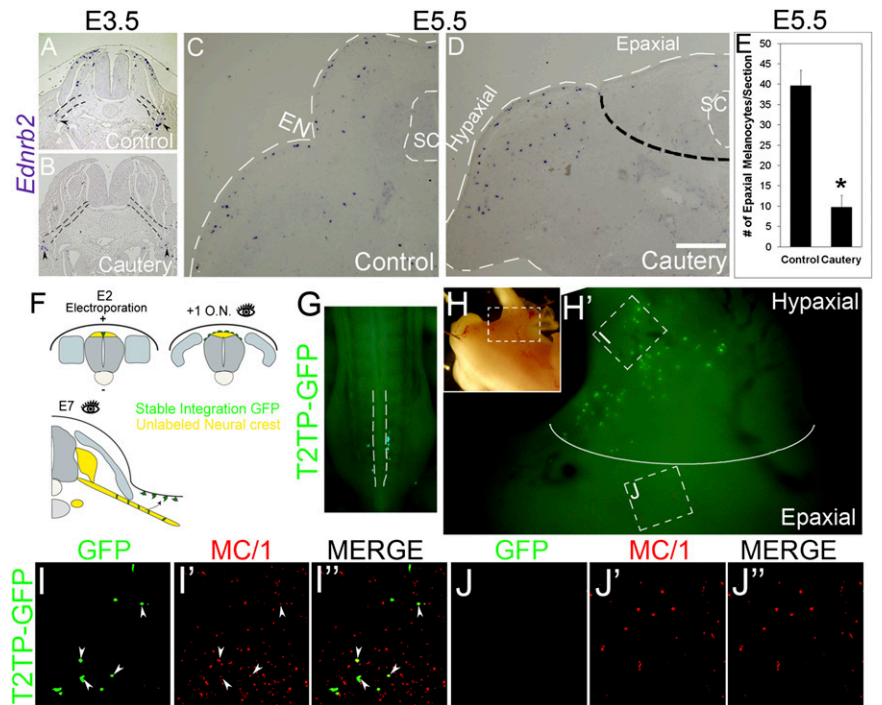


Fig. 1. Late-emigrating, NC-derived melanocytes populate the epaxial territory. (*A–D*) Electroporation of GFP-DNA into 35 ss embryos at the depicted axial levels. Note the position of the front of migrating cells 24 (*A*), 48 (*B*), and 72 (*C* and *D*) h after labeling. By 48 h, melanocytes reached the ectodermal notch (EN). (*D–D''*) The ventral limit of melanocyte colonization (arrowheads) coincides with that of *Sim1*, which delimits the somite-derived dermis from lateral plate-derived dermis. (*E* and *F*) ISH for *Ednrb2*. (*G* and *H*) Immunohistochemistry for *MC1* at E5. (*I* and *J*) Proportion (*I*) and density (*J*) of melanocytes in epaxial and hypaxial regions at limb and flank levels; $P < 0.05$ for hypaxial melanocytes at flank and limb levels, respectively. Density of epaxial melanocytes at hindlimb compared with flank was not significantly different ($P > 0.3$). EN, ectodermal notch; M, muscle; SC, spinal cord; SN, spinal nerve. (Scale bar, 50 μ m in *A* and *B*; 100 μ m in *C*, *D*, *D''*, *G*, and *H*; 70 μ m in *D'*; 200 μ m in *E* and *F*.)

SCP population) with GFP using Tol2 transposon-mediated genomic integration (19). Electroporation was performed at the hindlimb level of embryos aged 23 ss, before the onset of NC emigration. To selectively label the early emigrating cells, electric current was focally applied in a ventral to dorsal direction (Fig. 2*F*). Sixteen hours later, live embryos were inspected under a fluorescent stereoscope to ensure that all GFP⁺ cells emigrated (Fig. 2*G*) and that no residual labeling remained in the NT that at this stage still contained presumptive late-emigrating, NC-derived melanoblasts (5). Final analysis at E7 revealed that GFP⁺ cells were restricted to the hindlimbs where a subset coexpressed *MC1* ($n = 5$; Fig. 2*H* and *I–I''* and Fig. S1). In

Fig. 2. Early-emigrating, SCP-derived melanocytes colonize the hypaxial domain. (A–D) Indirect evaluation of the territory colonized by SCP-derived melanocytes. ISH for *Ednrb2* of intact embryos (A and C) and embryos whose dorsal NT was cauterized at 35 ss at the hindlimb level (B and D). (A and B) Twenty-four hours after cauterization, no *Ednrb2*⁺ cells are found in the dorsolateral pathway compared with intact controls. In contrast, note in both cases the presence of few ventral *Ednrb2*⁺ cells adjacent to the nerves (arrowheads). Black dotted lines in A and B delineate the spinal nerves. (C–E) At E5.5, *Ednrb2*⁺ melanocytes are found in both epaxial and hypaxial domains of control embryos but are missing in the epaxial domain of cauterized embryos. Dotted black line separates between epaxial and hypaxial (limb) domains. White dotted lines delimit the embryo surface and the spinal cord. (E) Quantification of the number of *Ednrb2*⁺ cells in the epaxial domain of E5.5 embryos, **P* < 0.05. (F–J) Direct visualization of SCP-derived melanocytes colonizing only the hypaxial limb territory. Stable and focal labeling of early emigrating NC cells that migrate along the ventral pathway to populate spinal nerves and other neural derivatives. (F) Experimental scheme. Ventral to dorsal coelectroporation of pCAGG-T2TP and pT2K-EGFP was performed at E2. Sixteen hours later, embryos were inspected to ensure that no residual GFP⁺ cells remained in the NT (i.e., that the prospective late emigrating NC-derived melanocytes are unlabeled; see also dorsal view of a living embryo in G). At E6–E7, the localization of GFP⁺ nerve-derived melanocytes cells was monitored (H–J’’, same embryo as in G). I and J are higher magnifications of the boxed areas in H/H’ representing the hypaxial limb (I–I’’) and epaxial (J–J’’) regions separated in H’ by a white line. Note that GFP⁺/MC1⁺ SCP-derived melanocytes (arrowheads in I–I’’) are restricted to the hypaxial domain. In contrast, NC-derived MC1⁺ epaxial melanocytes are GFP-negative (J and J’). Fig. S1 shows transverse sections. EN, epidermal notch; ON, overnight; SC, spinal cord. (Scale bar, 50 μm in A and B; 40 μm in C and D.)



contrast, MC1⁺ pigment cells in the epaxial domain were GFP-negative (Fig. 2H and J–J’’).

Altogether, NC-derived melanocytes migrate through the dermis and later invade the ectoderm as far ventral as the ectodermal notch, which represents the border between the epaxial and hypaxial body domains. Reciprocally, SCP-derived melanocytes are initially restricted to the hypaxial domain at wing and hindlimb regions, at least until E7. We cannot rule out the possibility that few melanocytes could derive from the dorsal ramus of the peripheral nerve and spread into the epaxial area. Even if this were the case, this does not undermine the significance of an epaxial vs. hypaxial segregation of melanocytes during the patterning phase, when these two subsets are first established. Previous experiments in chicken embryos in which GFP-labeled melanocytes were seen in the epaxial region could not discriminate between a direct NC vs. a dorsal ramus origin because labeling concerned the entire hemi-NT (9). Hence, during formation of the body plan, establishment of the epaxial/hypaxial border is relevant to the formation of distinct muscles (18, 20, 21) to the development of the epaxial dermis from the dermomyotome vs. the hypaxial dermis from the somatic layer of the lateral plate mesoderm (17, 22) and also to the restricted distribution of the two melanocyte subpopulations. The association between these processes is sensible because the dissociating dermal mesenchyme serves as substrate for melanoblast migration (23).

Foxd3 Acts as a Fate Switch Between SCPs and Hypaxial Melanocytes.

Foxd3 expression characterizes premigratory neural progenitors of the NC and early ventrally migrating cells (5, 14, 15), yet it is down-regulated in presumptive epaxial melanocytes before their exit from the NT (5, 8); at later organogenetic stages, *Foxd3* is down-regulated in DRG and SG neurons yet persists in glia and SCP for a few more days, until their final differentiation (refs. 14 and 15 and see below). Thus, we asked whether SCP-derived melanocytes express *Foxd3*. Cross-sections of E5 hindlimb segments

showed expression of *Foxd3* in cells along the spinal nerve (Fig. 3A). However, MC1⁺ cells surrounding the nerve were *Foxd3*-negative (Fig. 3B and C, arrowheads), suggesting that SCP-derived melanocytes down-regulate *Foxd3*. To examine whether hypaxial melanocytes derive from *Foxd3*⁺ SCPs, a previously characterized *Foxd3* enhancer element was cloned upstream of Cre recombinase and focally electroporated into the dorsal NT of avian embryos aged 22 ss along with a Cre-dependent GFP plasmid (*Foxd3*::Cre + pCAGG::LoxP-STOP-LoxP-GFP) (8), using the method described in Fig. 2F. This approach enabled stable lineage tracing of the enhancer expressing cells (8, 24, 25). Six hours after ventral to dorsal electroporation of NTs, GFP⁺ cells were restricted to the dorsal NT, where cells expressing endogenous *Foxd3* are located (8). Further analysis at E5 revealed the presence of GFP expression in both SCP along the nerve, as well as in MC1⁺ melanocytes in the limb (*n* = 5 of 6; Fig. 3D–F), corroborating the notion that SCP-derived hypaxial melanocytes, similar to their epaxial counterparts, stem from a *Foxd3*⁺ lineage.

Previous results demonstrated that misexpression of *Foxd3* in presumptive epaxial melanocytes inhibits their proper dorsolateral migration and differentiation while promoting instead a glial fate (8). Here we asked whether the SCP–melanocyte switch is similarly sensitive to *Foxd3*. To test this possibility, we prevented the normal down-regulation of *Foxd3* in SCP after they reached their final sites. To this end, full-length *Foxd3* under regulation of the tetracycline-responsive promoter (*Foxd3*-TRE) was electroporated into hindlimb-level hemitubes at 25 ss, along with rtTA2s-M2 (19). Two days later, when the transfected cells had reached the spinal nerve, doxycycline was injected underneath the blastoderm to induce *Foxd3* activity, and embryos were reincubated for an additional 24 h (Fig. 3G). In control GFP-TRE embryos, a subset of labeled cells lost contact with the nerve and up-regulated expression of MC1 and *Ednrb2* (*n* = 10; Fig. 3H–H’’, arrows, and Fig. S2A and B). In contrast, all *Foxd3*-TRE-GFP-transfected cells remained associated with the

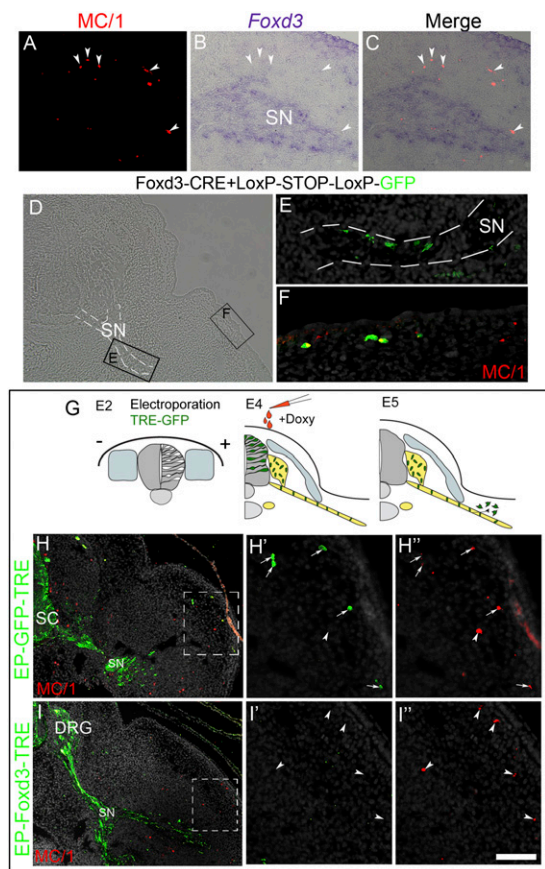


Fig. 3. Sustained *Foxd3* activity inhibits melanocyte differentiation of bipotent SCP-melanocyte progenitors. (A–C) Transverse section of an E5 limb showing nonoverlapping *Foxd3* and *MC1/1* signals in SCPs along a spinal nerve and melanocytes (arrowheads), respectively. (D–F) *MC1/1*⁺ melanocytes develop from *Foxd3*⁺ SCPs. Staining for *MC1/1* of a section through the hindlimb-level of an E5.5 embryo whose dorsal NT was focally electroporated at E2 with enhancer #168-cre and pCAGG::LoxP-STOP-LoxP-GFP. (E and F) Magnifications of boxed areas in D showing enhancer-positive cells along the nerve (E) and in the dermis/epidermis (F) where they coexpress *MC1/1*. Nerve is highlighted with dashed white lines. (G–I) Inducible expression of *Foxd3* in SCP along spinal nerves. (G) Experimental scheme: electroporation of pCAGGS-rtTA2s-M2 along with either pBI-TRE-GFP or pBI-TRE-*Foxd3* into hemi-NT at hindlimb levels of E2 embryos. Doxycycline was injected 2 d later, and the localization and fate of transfected cells was assessed at E5. In control embryos, *MC1/1*⁺ cells in the limb are GFP⁺ (arrows, H–H''), whereas *MC1/1*⁺ melanocytes in treated embryos are *Foxd3*/GFP-negative (arrowheads, I–I''). Doxy, doxycycline; SC, spinal cord. (Scale bar, 50 μ m in A–C; 70 μ m in D; 30 μ m in E and F; 80 μ m in H and I; 40 μ m in H'–H'' and I'–I'').

nerve and were *MC1/1* and *Ednrb2*-negative; reciprocally, the *Ednrb2* and *MC1/1*⁺ melanocytes in the hypaxial domain were *Foxd3*-GFP negative ($n = 7$, Fig. 3 I–I''), arrowheads, and Fig. S2 C and D). Quantifications revealed the presence of 3.1 ± 0.5 and 0.12 ± 0.1 GFP⁺/*MC1/1*⁺ melanocytes per section in control vs. *Foxd3*-treated conditions ($n = 4$ embryos and 18 sections counted for each treatment, $P < 0.01$). We conclude that both early migrating SCP as well as late-emigrating epaxial NC cells must down-regulate *Foxd3* for proper development into melanocytes.

Consistent with this notion, attenuation of *Foxd3* in vitro with antisense morpholinos enhanced melanogenesis (13, 26), and loss of *Foxd3* gene function in the mouse NC promoted melanocyte development at the expense of neural fates in DRG (8). To examine whether *Foxd3* similarly affects the balance between SCP and melanocytes in the mouse, we analyzed mouse embryos carrying a conditional deletion of *Foxd3* in the NC. We compared *Foxd3*^{lox/-}; *Wnt1-Cre*; *R26R* (mutant) embryos with *Foxd3*^{lox/+};

Wnt1-Cre; *R26R* (control) embryos. In the trunk of 12.5 days post-coitum (dpc) control embryos, growing nerves expressed *Tuj1*, and *Mitf*⁺ melanocytes were observed in the neighboring hypaxial dermis and ectoderm (Fig. 4 A and A'). In striking contrast, many *Mitf*⁺ cells were apparent along the mutant nerves in addition to their expected dermal/ectodermal distribution (Fig. 4 B and B'). Likewise, an ectopic up-regulation of *Mitf* was observed at 11.5 dpc along mutant cranial nerves compared with controls (Fig. 4 C and D). Together, these genetic data suggest that *Foxd3* is necessary for the maintenance of NC-derived SCP by repressing ectopic melanogenesis. Hence, both NC-derived epaxial and SCP-derived hypaxial melanoblasts require that *Foxd3* be down-regulated to correctly migrate and differentiate (Fig. 4E). Because enhanced melanogenesis was also reported to occur in mouse embryos lacking the neuregulin receptor *ErbB3* (9), we examined expression of *ErbB3* in *Foxd3* mutants. No apparent change in the pattern of *ErbB3* expression could be detected in SCPs along mutant compared with control nerves (Fig. S3). Reciprocally, no dependency of *Foxd3* expression on *ErbB3* was detected (10), altogether indicating that each gene independently affects the SCP-melanocyte balance in the nerve environment. Nevertheless, less *ErbB3* expression was observed in mutant compared with control DRG at 11.5 and 12.5 dpc (Fig. S3), likely reflecting the previously observed reduction in glial cell number associated with a glial-to-melanocyte switch (8).

Foxd3 Acts as a Fate Switch Between Neurons and Glia in the DRG.

Next, we examined whether *Foxd3* activity is involved in fate decisions of additional NC derivatives. Although ventrally migrating NC progenitors transcribe *Foxd3* (5, 14, 15), differentiating sensory neurons in nascent DRG, marked by expression of *ISLET1*, down-regulate *Foxd3* mRNA (Fig. 5A). However, many *Fabp7*⁺ glial cells as well as undifferentiated progenitors (*ISLET1*⁻/*Fabp7*⁺) still maintain *Foxd3* expression [Fig. 5 B–B''] (15). We therefore hypothesized that preventing *Foxd3* down-regulation in differentiating DRG will inhibit neuronal differentiation while respecifying them into glia as previously shown (see above and ref. 8) and/or maintaining them in a progenitor state (15, 27, 28).

Foxd3-TRE was electroporated into the E2 chick NT as shown in Fig. 3G. Thirty hours later, when migrating NC cells have begun colonizing the DRG, doxycycline was supplied and embryos reincubated for another day. At E4, control GFP-TRE⁺ cells were distributed throughout the ganglion where they coexpressed

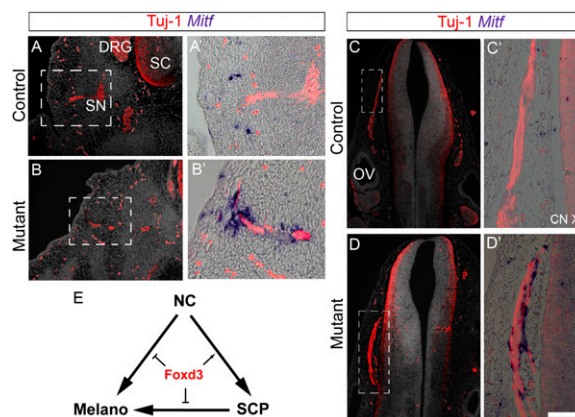


Fig. 4. Enhanced melanogenesis in mutant mouse embryos lacking *Foxd3* in the NC. (A–D) Staining for *Mitf* and *Tuj-1* in sections through spinal nerves (A and B) and cranial accessory nerves (C and D) of 12.5 dpc (A and B) and 11.5 dpc (C and D) control and mutant mouse embryos. Note ectopic *Mitf*⁺ cells closely associated to the nerves in mutant mice. (E) Model summarizing the role of *Foxd3* in melanocytes emanating either directly from the NC or indirectly from NC-derived SCPs. CN, cranial nerve; OV, otic vesicle; SC, spinal cord. (Scale bar, 50 μ m in A and B; 30 μ m in A', B', C', and D'; 70 μ m in C and D.)

Materials and Methods

Embryos. *Avian embryos.* Chick (*Gallus gallus*) eggs were obtained from commercial sources. Experiments were conducted either in forelimb, hindlimb, or midtrunk level as indicated.

Mouse embryos. The *Foxd3* conditional and null alleles (*Foxd3^{fllox}* and *Foxd3^{-/-}*) were described previously (28, 31). The *Wnt1-Cre* transgenic line was used to delete *Foxd3^{fllox}* in the NC (*Foxd3^{fllox/-}; Wnt1-Cre* mutant embryos), and to lineage map NC, the R26R^{YFP} reporter strain was used (29).

Expression Vectors. The following vectors were used: pCAGG-AFP, pCAGG-RFP, the *Foxd3* enhancer element 168-Cre, pCAGG::LoxP-STOP-LoxP-GFP (8), pT2K-CAGGS-EGFP and pCAGGS-T2TP (19), and pBI-TRE-GFP and pBI-TRE-*Foxd3* along with pCAGGS-rtTA2s-M2 (see below and ref. 32).

Lineage Analysis of *Foxd3*-Expressing Cells Along Spinal Nerves. A plasmid containing the #168 enhancer from the Vista enhancer browser (<http://enhancer.lbl.gov>) driving expression of Cre recombinase was coelectroporated into dorsal NT along with a reporter plasmid in which a floxed transcriptional STOP module was inserted between the CAGG enhancer/promoter and the GFP gene (pCAGG::LoxP-STOP-LoxP-GFP) (25, 33).

Tetracyclin-Induced Expression of *Foxd3*. Full-length chick *Foxd3* was cloned into pBI (pTRE) and coelectroporated along with pCAGGS-rtTA2s-M2 into hemi-NTs at the hindlimb level of 25 ss embryos. Embryos were inspected under epifluorescence to monitor for possible signal leakage at 24 or 48 h after electroporation; doxycycline was then injected underneath the blastoderm, as previously described (32). Embryos were reincubated for additional 12–24 h before fixation.

Embryo Manipulations. Electroporation. Plasmid DNA (2–5 mg/mL) was microinjected into the lumen of the chick NT. For hemi-NT electroporations, 0.5-mm tungsten electrodes were placed on either side of the embryo. For focal

electroporations of the dorsal NT, a 5-mm L-shaped tungsten electrode was placed underneath the blastoderm, with a pointed electrode dorsal to the desired region. A square wave electroporator (BTX, Inc.) was used to deliver one to two pulses of current at 10–25 V for 10 ms.

Cautery. The dorsal portion of the NT was cauterized at the hindlimb level of embryos aged 35 ss using a standard animal cauterization kit (Bovie). One and twenty-four hours later, embryos were analyzed to assess for the specificity of the procedure and further reincubated until E5.5.

Immunohistochemistry and in Situ Hybridization. Antibodies against HNK1 (CD57; BD Biosciences), GFP (Invitrogen), MC1 (5, 34), Brn3a (Chemicon), and ISLET-1 (Hybridoma Bank) were used as previously described (35). Cell nuclei were visualized with Hoechst.

In situ hybridization (ISH) was performed as previously described (36). The following probes were used: chick *Foxd3* (14, 15), *Sim1* (17), *Ednrb2* (8), *Fabp7* (37), *Hmx1* (9), and mouse *Mitf* (38) and *ErbB3* (39).

Data Analysis and Statistics. The relative percentages of epaxial vs. hypaxial melanocytes expressing either MC1 or *Ednrb2*, the number of melanocytes per unit area, and the percentage of ISLET⁺ of total GFP⁺ neurons in DRG were monitored. Results represent mean ± SEM of 5–10 sections per embryo counted in 4–8 embryos per experimental treatment. An average of 4–15 melanocytes per section was counted in the different domains. Data were subjected to statistical analysis using the nonparametric Mann-Whitney and Kruskal-Wallis tests. All tests applied were two-tailed with *P* ≤ 0.05.

ACKNOWLEDGMENTS. We thank Yoshiko Takahashi, Avihu Klar, Makoto Mochii, Carmen Birchmeier, Thomas Muller, Martin Wegner, and Patrick Ernoffs for reagents. This work was supported by Deutsche Forschungsgemeinschaft Grant UN34/27-1, Association Francaise contre les Myopathies Grant 15642, and Israel Science Foundation Grant 11/09 (to C.K.), and National Institutes of Health Grant HD36720 and American Heart Association Grant 11GRNT7690040 (to P.A.L.).

- García-Castro M, Bronner-Fraser M (1999) Induction and differentiation of the neural crest. *Curr Opin Cell Biol* 11(6):695–698.
- Le Douarin NM, Kalchauer C (1999) *The Neural Crest* (Cambridge Univ Press, New York), 2nd Ed.
- Adameyko I, Lallemand F (2010) Glial versus melanocyte cell fate choice: Schwann cell precursors as a cellular origin of melanocytes. *Cell Mol Life Sci* 67(18):3037–3055.
- Krispin S, Nitzan E, Kalchauer C (2010) The dorsal neural tube: A dynamic setting for cell fate decisions. *Dev Neurobiol* 70(12):796–812.
- Krispin S, Nitzan E, Kassem Y, Kalchauer C (2010) Evidence for a dynamic spatiotemporal fate map and early fate restrictions of premigratory avian neural crest. *Development* 137(4):585–595.
- Serbedzija GN, Bronner-Fraser M, Fraser SE (1989) A vital dye analysis of the timing and pathways of avian trunk neural crest cell migration. *Development* 106(4):809–816.
- Erickson CA, Reedy MV (1998) Neural crest development: The interplay between morphogenesis and cell differentiation. *Curr Top Dev Biol* 40:177–209.
- Nitzan E, et al. (2013) A dynamic code of dorsal neural tube genes regulates the segregation between neurogenic and melanogenic neural crest cells. *Development* 140(11):2269–2279.
- Adameyko I, et al. (2009) Schwann cell precursors from nerve innervation are a cellular origin of melanocytes in skin. *Cell* 139(2):366–379.
- Adameyko I, et al. (2012) Sox2 and Mitf cross-regulatory interactions consolidate progenitor and melanocyte lineages in the cranial neural crest. *Development* 139(2):397–410.
- Dupin E, Le Douarin NM (2003) Development of melanocyte precursors from the vertebrate neural crest. *Oncogene* 22(20):3016–3023.
- Real C, Glavieux-Pardanaud C, Le Douarin NM, Dupin E (2006) Clonally cultured differentiated pigment cells can dedifferentiate and generate multipotent progenitors with self-renewing potential. *Dev Biol* 300(2):656–669.
- Thomas AJ, Erickson CA (2009) FOXD3 regulates the lineage switch between neural crest-derived glial cells and pigment cells by repressing MITF through a non-canonical mechanism. *Development* 136(11):1849–1858.
- Kos R, Reedy MV, Johnson RL, Erickson CA (2001) The winged-helix transcription factor *Foxd3* is important for establishing the neural crest lineage and repressing melanogenesis in avian embryos. *Development* 128(8):1467–1479.
- Dottori M, Gross MK, Labosky P, Goulding M (2001) The winged-helix transcription factor *Foxd3* suppresses interneuron differentiation and promotes neural crest cell fate. *Development* 128(21):4127–4138.
- Olivera-Martinez I, Coltey M, Dhouailly D, Pourquie O (2000) Mediolateral somitic origin of ribs and dermis determined by quail-chick chimeras. *Development* 127(21):4611–4617.
- Ben-Yair R, Kahane N, Kalchauer C (2003) Coherent development of dermomyotome and dermis from the entire mediolateral extent of the dorsal somite. *Development* 130(18):4325–4336.
- Cheng L, Alvarez LE, Ahmed MU, El-Hanfy AS, Dietrich S (2004) The epaxial-hypaxial subdivision of the avian somite. *Dev Biol* 274(2):348–369.
- Sato Y, et al. (2007) Stable integration and conditional expression of electroporated transgenes in chicken embryos. *Dev Biol* 305(2):616–624.
- Huang R, Christ B (2000) Origin of the epaxial and hypaxial myotome in avian embryos. *Anat Embryol (Berl)* 202(5):369–374.
- Ordahl CP, Le Douarin NM (1992) Two myogenic lineages within the developing somite. *Development* 114(2):339–353.
- Christ B, Scaal M (2008) Formation and differentiation of avian somite derivatives. *Adv Exp Med Biol* 638:1–41.
- Nitzan E, Kalchauer C (2013) Neural crest and somitic mesoderm as paradigms to investigate cell fate decisions during development. *Dev Growth Differ* 55(1):60–78.
- Zisman S, et al. (2007) Proteolysis and membrane capture of F-spondin generates combinatorial guidance cues from a single molecule. *J Cell Biol* 178(7):1237–1249.
- Avraham O, et al. (2009) Transcriptional control of axonal guidance and sorting in dorsal interneurons by the Lim-HD proteins Lhx9 and Lhx1. *Neural Dev* 4:21.
- Thomas AJ, Erickson CA (2008) The making of a melanocyte: The specification of melanoblasts from the neural crest. *Pigment Cell Melanoma Res* 21(6):598–610.
- Nelms BL, Labosky PA (2010) *Transcriptional Control of Neural Crest Development* (Morgan & Claypool Life Sciences, San Rafael, CA).
- Hanna LA, Foreman RK, Tarasenko IA, Kessler DS, Labosky PA (2002) Requirement for *Foxd3* in maintaining pluripotent cells of the early mouse embryo. *Genes Dev* 16(20):2650–2661.
- Mundell NA, Labosky PA (2011) Neural crest stem cell multipotency requires *Foxd3* to maintain neural potential and repress mesenchymal fates. *Development* 138(4):641–652.
- Wakamatsu Y, Maynard TM, Weston JA (2000) Fate determination of neural crest cells by NOTCH-mediated lateral inhibition and asymmetrical cell division during gangliogenesis. *Development* 127(13):2811–2821.
- Teng L, Mundell NA, Frist AY, Wang Q, Labosky PA (2008) Requirement for *Foxd3* in the maintenance of neural crest progenitors. *Development* 135(9):1615–1624.
- Watanabe T, et al. (2007) Tet-on inducible system combined with in ovo electroporation dissects multiple roles of genes in somitogenesis of chicken embryos. *Dev Biol* 305(2):625–636.
- Timmer J, Johnson J, Niswander L (2001) The use of in ovo electroporation for the rapid analysis of neural-specific murine enhancers. *Genesis* 29(3):123–132.
- Mochii M, Takeuchi T, Kodama R, Agata K, Eguchi G (1988) The expression of melanosomal matrix protein in the transdifferentiation of pigmented epithelial cells into lens cells. *Cell Differ* 23(1-2):133–141.
- Burstyn-Cohen T, Kalchauer C (2002) Association between the cell cycle and neural crest delamination through specific regulation of G1/S transition. *Dev Cell* 3(3):383–395.
- Shoval I, Ludwig A, Kalchauer C (2007) Antagonistic roles of full-length N-cadherin and its soluble BMP cleavage product in neural crest delamination. *Development* 134(3):491–501.
- Kang P, et al. (2012) Sox9 and NFIA coordinate a transcriptional regulatory cascade during the initiation of gliogenesis. *Neuron* 74(1):79–94.
- Stolt CC, Lommes P, Hillgärtner S, Wegner M (2008) The transcription factor Sox5 modulates Sox10 function during melanocyte development. *Nucleic Acids Res* 36(17):5427–5440.
- Britsch S, et al. (1998) The ErbB2 and ErbB3 receptors and their ligand, neuregulin-1, are essential for development of the sympathetic nervous system. *Genes Dev* 12(12):1825–1836.